PHYSICAL REVIEW B VOLUME 45, NUMBER 16 15 APRIL 1992-II

Metastable energy distribution and localization of spatially indirect excitons

J. E. Golub
Racah Institute of Physics, The Hebrew University of Jerusalem, Jerusalem, Israel

K. Kash, J. P. Harbison, and L. T. Florez
Bellcore, 331 Newman Springs Road, Red Bank, New Jersey 07701-7040

(Received 18 November 1991)

We report the electric-field-induced localization of extremely-long-lived excitons, with lifetimes of up to 5 μs, in coupled GaAs/$Al_xGa_{1-x}As$ quantum wells. The effect is manifested in a field-sensitive temperature dependence of the exciton recombination time that is well fit by a model based on a field-dependent mobility edge. The observed field dependence of the exciton through the transition from a mobile to a localized gas is consistent with an exciton gas that is in metastable equilibrium, and is not consistent with either a Bose distribution or with a spatial distribution dominated by dipole-dipole repulsion.

Much recent work has sought to illuminate the nature of exciton motion in single quantum wells.[1-11] These studies have focused on the problem of localization in two dimensions, energy dynamics of excitons, the role of phonons, and new optical probes of heterointerface quality. The picture which has gradually emerged from these works includes the following elements: (1) At low temperatures, excitons may be localized by random potential fluctuations associated with heterointerface roughness. (2) Excitons may undergo spatial diffusion mediated by acoustic-phonon scattering and defect scattering. An important limitation in these experiments has been the time scale: Motion can only be observed over the time scale of the recombination lifetime of the exciton. In single quantum-well structures of high-quality material, the measurement time has been thus limited to approximately 1 ns.

In this work, we return to the basic questions of exciton motion, but on a different time scale. By studying the long-lived spatially indirect exciton of a double quantum well,[12,13] we gain information about exciton motion on the time scales as long as 5 μs, an increase of nearly 4 orders of magnitude over that available in single quantum-well samples. Our principal results are (1) a persistence of the inhomogeneously broadened emission line to the longest time scales, strong evidence that the system is in metastable equilibrium; and (2) an electric-field-induced transition from a regime in which the recombination lifetime is quite sensitive to temperature, characteristic of a mobile exciton gas, to a high-field regime in which the lifetime is independent of temperature.

Early work on coupled quantum wells, based on optical spectroscopy and simple calculations, dealt with the character of the exciton in coupled wells.[14-16] A particular finding was the possibility to electric-field-tune the exciton from a spatially direct excitation characterized by large overlap of electron and hole wave functions and a vanishing electric dipole moment, to a spatially indirect object characterized by small overlap and large dipole moment. The transition between these two regimes is mediated by a tunneling-induced level anticrossing with an interesting device potential.[16] In the case of spatially indirect excitons, the recombination lifetime is greatly increased owing to the reduced electron-hole overlap.[12,13] At the same time, the dipole moment of spatially indirect excitons is enhanced as the spatial separation is increased, and can be as large as $300ea_0$ (e is the electron charge, a_0 is the hydrogen Bohr radius) owing to the spatial separation of the electron and the hole.[17]

In this work, we present the results of time-integrated and time-resolved measurements of photoluminescence (PL) in coupled GaAs/$Al_xGa_{1-x}As$ quantum wells over a range of temperatures and electric fields. The GaAs/$Al_{0.3}Ga_{0.7}As$ sample used was grown by molecular-beam epitaxy, and has been described in detail elsewhere.[13] Briefly, the structure consists of a single pair of GaAs quantum wells (10.0 and 15.0 nm nominal layer thickness) separated by an $Al_{0.3}Ga_{0.7}As$ barrier of thickness 3.0 nm. The coupled well unit lies at the center of the 1-μm thick intrinsic layer of a p-i-n diode. At flat band, ground-state electrons and holes are each confined in the 15.0-nm quantum-well layer and the resulting exciton is spatially direct. Under reverse bias, the ground state of the hole continues to be confined to the 15.0-nm well, while the ground state of the electron is separately confined to the 10.0-nm well layer. The resulting exciton is spatially indirect. The sample was held at low temperature by immersion in liquid helium or a bath of helium gas, and could be cooled to an ultimate temperature of 2.1 K. The experiments were performed using picosecond pulsed optical excitation and delayed coincidence photon counting techniques. The synchronously pumped rhodamine 6G laser was tuned to 590 nm and cavity dumped at repetition rates as slow as 40 kHz in order to accommodate the very-long-lived luminescence signals. For the pulse energies used here, we estimate the exciton density to be 1×10^9 cm^{-2}. Time-resolved PL traces were recorded by widening the spectrometer slits to spectrally integrate over the entire emission line.

Figure 1 shows the observed development of the PL decay time with electric field. The lifetime rises nearly exponentially over the range 9–30 kV/cm. At higher fields,

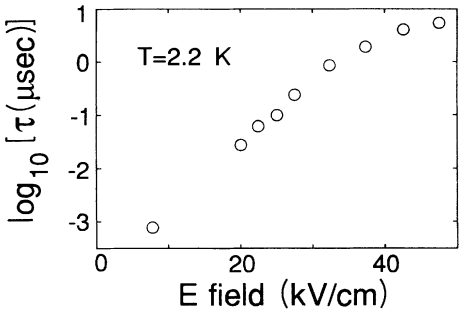

FIG. 1. The electric-field dependence of the photoluminescence lifetime at $T=2.2$ K.

the lifetime exhibits a saturating behavior, and reaches a value of approximately 5 μs. This very large enhancement of the lifetime with electric field—4 orders of magnitude—agrees with a simple particle-in-a-box calculation of the electron-hole overlap. Physically, as the electron and the hole are drawn toward opposite sides of the quantum well by the electric field, the wave-function overlap drops, and with it the recombination rate. This interpretation holds for both radiative and nonradiative recombination.

Figure 2 shows the full width at half maximum (FWHM) of the time-integrated PL spectrum (open circles), recorded at $T=2.2$ K. The most prominent feature in the data is the sharp rise in the linewidth from its near-flat-band value of 0.68–2.3 meV at an electric field of 14 kV/cm. This behavior is consistent with the standard picture of inhomogeneous broadening of quantum-well excitons due to well width fluctuations. According to this picture, the inhomogeneous linewidth for a single, infinite quantum well is determined by

$$\Delta=\frac{\partial E}{\partial L}\Delta L\sim\frac{1}{L^3}, \tag{1}$$

where $E=\pi^2\hbar^2/2\mu L^2$ is the exciton confinement energy in the approximation of an infinite well, μ is the reduced mass, and ΔL is a characteristic well width fluctuation. We consider first the near-flat-band situation in which both the electron and the hole are confined to the 15-nm quantum-well layer. Assuming monolayer fluctuations on the inverted (GaAs on $Al_xGa_{1-x}As$) interface and half-monolayer (ML) fluctuations on the normal ($Al_xGa_{1-x}As$ on GaAs) interface, we compute $\Delta L=[(1\ \mathrm{ML})^2+(\frac{1}{2}\ \mathrm{ML})^2]^{1/2}=0.32$ nm, where 1 ML = 0.283 nm is the monolayer thickness. The inhomogeneous broadening of the exciton energy is then computed from Eq. (1) as $\Delta=0.6$ meV, in good agreement with the observed value of 0.68 meV.

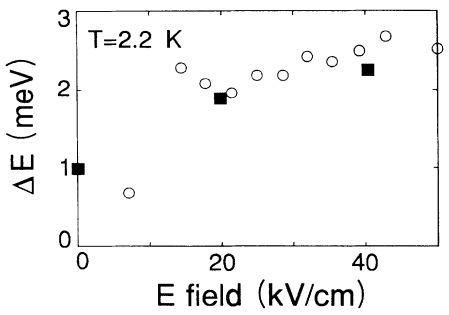

FIG. 2. The electric-field dependence of the linewidth (FWHM) of time-integrated photoluminescent emission. The solid squares are the result of a model described in the text.

In passing to the case of the spatially indirect exciton, we must modify the standard model to take into account the separate confinement of the electron and the hole. We thus consider two terms of the form of Eq. (1), and write

$$\Delta^2=\left(\frac{\partial E_e}{\partial L_e}\Delta L_e\right)^2+\left(\frac{\partial E_h}{\partial L_h}\Delta L_h\right)^2 \tag{2}$$

where the subscripts indicate the confinement energies and well widths appropriate to the electron or the hole. With the electron confined to the 10-nm well, and the hole confined to the 15-nm well, we calculate $\Delta=1.8$ meV, a factor of 3 larger than the near-flat-band case. This factor of 3 broadening is in excellent agreement with the data of Fig. 2. Thus, we have explained the sudden rise in PL linewidth at 14 kV/cm in the data of Fig. 2.

We show next that the observed slow rise in photoluminescence linewidth for electric fields greater than 14 kV/cm is also consistent with the standard picture of inhomogeneous broadening. We calculate the distribution of exciton energies due to interfacial roughness using a static model. In our model, deviations of the real interface positions from the ideal are normally distributed with a width which characterizes the magnitude of the disorder. For the two normal interfaces we again assume a distribution with half width at half maximum $\frac{1}{2}$ ML. For the inverted interfaces, we assume a half width of 1 ML. The disorder at each of the four heterointerfaces is taken to be uncorrelated. We compute the change in the energy due to such deviations using a particle-in-a-box calculation incorporating the electric field. Finally, we use standard Monte Carlo techniques to build a model disordered crystal and to evaluate the distribution of exciton energies throughout the crystal. The solid squares in Fig. 2 give the results of this calculation. Importantly, the model and data both indicate an increase in the degree of disorder with increasing electric field. There are thus two effects associated with the applied electric field: a reduction in the electron-hole wave-function overlap and an increase in the degree of disorder of the system.

We next show that the data of Fig. 2 imply a metastable energy distribution. We consider a thermal gas of excitons and take into account the presence of well width fluctuations. The emission line shape in this system is determined by

$$g(E)\propto f(E)\rho(E), \tag{3}$$

where $f(E)$ is the exciton energy distribution function and $\rho(E)$ is the density of states. We have assumed an energy-independent transition rate. We assume first a Bose distribution in the exciton energies. In the absence of sharp features in the density of states function $\rho(E)$, Eq. (3) predicts a linewidth $\Delta E\approx kT$. By contrast, the

observed linewidths range around 2 meV, a factor of 12 higher than the sample temperature (2.1 K). We conclude that the exciton gas is not well described by an equilibrium Bose distribution, consistent with the findings of Ref. 18.

We consider instead a Fermi-Dirac distribution. Such a distribution was recently used to account for the dipole-dipole interaction in a gas of spatially indirect excitons.[18] The use of the Fermi-Dirac distribution in this instance is based on the hypothesis that two spatially indirect excitons do not occupy the same site because of dipole-dipole repulsion. We estimate the area occupied by a single exciton by equating the dipole-dipole energy with the thermal energy,

$$(e^2/\epsilon a)(a/l_{\min})^3 = kT . \quad (4)$$

Here, a is the mean electron-hole distance, $l_{\min}$ is the exciton-exciton separation, and ϵ is the dielectric constant. For the temperature of our experiments (2.1 K), we can compute the minimum interexciton distance $l_{\min}$ from Eq. (4), and estimate the density of localized sites as $\sigma = 1/\pi l_{\min}^2$. We find $\sigma = 8\times10^{10}$ cm^{-2}. As noted above, the initial exciton density in our experiments is approximately 1×10^9 cm^{-2}. Under these circumstances, we may rule our state filling, and conclude that Fermi statistics also do not provide an adequate description of these data.

We suggest instead that the linewidths of Fig. 2 are consistent with the localization of spatially indirect excitons. In this picture, excitons are bound to local sites, and the intersite transfer time is long compared to the lifetime of the exciton. In the present case, the conclusion is especially striking because of the greatly enhanced lifetime. The data indicate energy relaxation of the exciton gas on time scales long compared with the longest lifetime observed—approximately 5 μs.

Simple kinematic considerations may offer the explanation for this metastability. Consider a gas of spatially indirect excitons whose kinetic energy of motion reflects thermal equilibrium with the lattice (temperature T), but whose potential energy is distributed over a range ΔE in accordance with localized site energies. In hopping to a lower energy site, an exciton would emit an acoustic phonon with energy ΔE. This implies a loss of momentum by the exciton of $\Delta p = \Delta E/c_s$, where c_s is the speed of sound. However, the initial exciton momentum may be estimated as $p_0 = (MkT)^{1/2}$. We take $\Delta E = 2$ meV, the photoluminescence linewidth, $c_s = 3\times10^3$ m/s, and $M = 0.45m_0 + 0.067m_0 = 0.52m_0$, and compute $\Delta p/p_0 = 42/T^{1/2}$, where T is the temperature in kelvin. Thus, for the temperatures studied here, acoustic-phonon emission over the energy range necessary for hopping is frozen out.

We next studied the temperature dependence of the radiative lifetime. Figure 3 shows the observed variation of lifetime with sample temperature for several values of applied electric field. For weak fields, the lifetime rises rapidly with increasing temperature, achieving an enhancement of 25 times over the temperature range 2.2–20 K. With increasing field strength, the temperature dependence weakens until, at fields of 35–40 kV/cm, the lifetime becomes independent of temperature over the range observed. The data are consistent with a picture based on

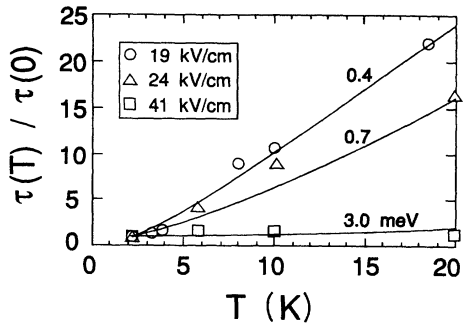

FIG. 3. The computed and observed temperature dependence of the lifetime enhancement for several electric fields. The computed curves are labeled by the position of the mobility edge with respect to the ground state of the disordered model crystal.

exciton localization. Mobile excitons exhibit a strongly temperature-dependent lifetime as a result of the requirement of conservation of center-of-mass momentum.[19,20] Recombination is momentum-allowed only within a homogeneous linewidth of the bottom of the exciton band. With increasing temperatures, progressively fewer excitons satisfy this rule, and the lifetime of the exciton gas increases. By contrast, recombination is allowed for all localized excitons. Therefore, when the interaction with the disorder is relatively weak, as in the case of weak electric fields, most excitons are mobile and the gas exhibits a temperature-dependent lifetime. With increasing electric field, the localized fraction grows at the expense of the mobile fraction, and the temperature dependence of the lifetime decreases. When the exciton gas is entirely localized, the temperature dependence vanishes.

We may use these ideas to model the data of Fig. 3 according to

$$\frac{\tau_0}{\tau_{\rm eff}(T)} = f_{\rm loc}\left[\frac{\tau_0}{\tau_{\rm loc}}\right] + (1-f_{\rm loc})\left[\frac{\tau_0}{\tau_{\rm mob}(T)}\right] . \quad (5)$$

Here, $\tau_{\rm eff}(T)$ is the observed lifetime, $\tau_{\rm loc}$ is the lifetime of localized excitons, $\tau_{\rm mob}$ is the lifetime of mobile excitons, $f_{\rm loc}$ gives the fraction of excitons localized, and τ_0 normalizes the results to the low-temperature effective lifetime. According to the treatment of Ref. 19, the temperature dependence of the free-exciton lifetime is given by

$$\tau/\tau_{\rm mob}(T) = (1-e^{-\Delta/kT})^{-1} , \quad (6)$$

where Δ is the homogeneous width of the exciton transition. We have ignored the temperature dependence of the homogeneous width, as this effect is dominated by $f_{\rm loc}(T)$. We also ignore in the present work the possibility of a giant oscillator strength of localized excitons, and set $\tau_{\rm loc}/\tau_0 = 1$. Finally, we assume the temperature dependence of $f_{\rm loc}$ to be determined by thermal activation of a classical exciton gas beyond a mobility edge, and write

$$f_{\rm loc}(\mu,T) = \int^{\mu} dE'\rho(E')e^{-E'/kT} , \quad (7)$$

where $\rho(E)$ is the disorder-dependent density of states and μ gives the energy of the mobility edge with respect to the ground state. Choosing a particular form for the

density-of-states function, we may calculate $f_{loc}(T)$. Combining those results with Eqs. (5) and (6), we find the temperature dependence of the lifetime enhancement for various values of μ. The results of three such calculations are shown in Fig. 3. The graphs show that the temperature dependence of the lifetime is well accounted for by a field-dependent shift of the mobility edge.

Our temperature data may also be explained as a temperature-dependent homogeneous broadening rate within the framework of Ref. 19. However, this picture would require a homogeneous linewidth large compared to kT_{max}, where $T_{max}=20$ K. Such a width would be large compared to the observed spectral width of 2 meV, an unphysical result.

Finally, we note that a disorder-induced giant oscillator strength has been discussed,[20] similar to the giant oscillator effect of impurity-bound excitons.[21,22] The treatment given above based on Eq. (1) ignores this possibility in the interest of simplicity. However, Eq. (1) may offer a framework for studying this interesting effect using strictly linear optics. Further experiments should help to clarify this issue.

In conclusion, we have observed the metastable energy distribution of a gas of spatially indirect excitons to times as long as 5 μs. The metastable distribution is inconsistent with a picture based on dipole-dipole repulsion and site filling. However, simple kinematic arguments suggest that the freezing out of acoustic-phonon emission—and hence intersite transfer—may explain the phenomenon. The localization picture is strongly supported by studies of the temperature dependence of the recombination lifetime.

[1]J. Hegarty, L. Goldner, and M. D. Sturge, Phys. Rev. B **30**, 7346 (1984).

[2]J. Hegarty and M. D. Sturge, J. Opt. Soc. Am. B **2**, 1143 (1985).

[3]T. Takagahara, Phys. Rev. B **32**, 7013 (1985).

[4]H. Sakaki, T. Noda, K. Hirakawa, M. Tanaka, and T. Matsusue, Appl. Phys. Lett. **51**, 1934 (1987).

[5]R. Gottinger, A. Gold, G. Abstreiter, G. Weiman, and W. Schlapp, Europhys. Lett. **6**, 183 (1988).

[6]T. Takagahara, J. Lumin. **44**, 347 (1989).

[7]C. Weisbuch, R. Dingle, A. C. Gossard, and W. Wiegman, Solid State Commun. **38**, 709 (1981).

[8]H. Hillmer, S. Hansmann, A. Forchel, M. Morohashi, E. Lopez, H. P. Meier, and K. Ploog, Appl. Phys. Lett. **53**, 1937 (1988).

[9]K. T. Tsen, O. F. Sankey, and H. Morkoc, Appl. Phys. Lett. **57**, 1666 (1990).

[10]Ch. Maierhofer, S. Munnix, D. Bimberg, R. K. Bauer, D. E. Mars, and J. N. Miller, Appl. Phys. Lett. **55**, 50 (1989).

[11]H. Matsueda and K. Hara, Appl. Phys. Lett. **55**, 362 (1989).

[12]S. Charbonneau, M. L. W. Thewalt, Emil S. Koteles, and B. Elman, Phys. Rev. B **38**, 6287 (1988).

[13]J. E. Golub, K. Kash, J. P. Harbison, and L. T. Florez, Phys. Rev. B **41**, 8564 (1990).

[14]Y. J. Chen, E. S. Koteles, B. S. Elman, and C. A. Armiento, Phys. Rev. B **36**, 4562 (1987).

[15]H. Q. Le, J. J. Zayhowski, and W. D. Goodhue, Appl. Phys. Lett. **50**, 1518 (1987).

[16]J. E. Golub, P. F. Liao, D. J. Eilenberger, J. P. Harbison, L. T. Florez, and Yehiam Prior, Appl. Phys. Lett. **53**, 2584 (1988).

[17]F. M. Peeters and J. E. Golub, Phys. Rev. B **43**, 5159 (1991).

[18]J. Kash, M. Zachau, E. E. Mendez, J. M. Hong, and T. Fukuzawa, Phys. Rev. Lett. **66**, 2247 (1991).

[19]J. Feldmann, G. Peter, E. O. Gobel, P. Dawson, K. Moore, C. Foxon, and R. J. Elliott, Phys. Rev. Lett. **59**, 2337 (1987).

[20]G. W. 't Hooft, W. A. J. A. van der Poel, L. W. Molenkamp, and C. T. Foxon, Phys. Rev. B **35**, 8281 (1987).

[21]T. Takagahara and E. Hanamura, Phys. Rev. Lett. **56**, 2533 (1986).

[22]E. I. Rashba and G. E. Gurgenishvili, Fiz. Tverd. Tela (Leningrad) **4**, 1029 (1962) [Sov. Phys. Solid State **4**, 759 (1962)].